Direct synthesis of well-defined zwitterionic cyclodextrin polymers via atom transfer radical polymerization

Diget, Jakob Stensgaard; Städe, Lars Wagner; Nielsen, Thorbjørn Terndrup

Published in:
European Polymer Journal

DOI (link to publication from Publisher):
10.1016/j.eurpolymj.2019.03.020

Publication date:
2019

Document Version
Accepted author manuscript, peer reviewed version

Accepted Manuscript

Direct synthesis of well-defined zwitterionic cyclodextrin polymers via atom transfer radical polymerization

Jakob Stensgaard Diget, Lars Wagner Städe, Thorbjørn Terndrup Nielsen

PII: S0014-3057(18)32027-5
DOI: https://doi.org/10.1016/j.eurpolymj.2019.03.020
Reference: EPJ 8922

To appear in: *European Polymer Journal*

Received Date: 9 November 2018
Revised Date: 13 February 2019
Accepted Date: 8 March 2019

Please cite this article as: Stensgaard Diget, J., Wagner Städe, L., Terndrup Nielsen, T., Direct synthesis of well-defined zwitterionic cyclodextrin polymers via atom transfer radical polymerization, *European Polymer Journal* (2019), doi: https://doi.org/10.1016/j.eurpolymj.2019.03.020

Direct synthesis of well-defined zwitterionic cyclodextrin polymers via atom transfer radical polymerization

Jakob Stensgaard Diget,[a,b,*] Lars Wagner Städe[c] and Thorbjørn Terndrup Nielsen[c,*]

a. Department of Chemistry, University of Oslo, P.O. Box 1033, Blindern, N-0315 Oslo, Norway. **b.** Jotun A/S, Hystadveien 167, N-3209 Sandefjord, Norway. **c.** Department of Chemistry and Bioscience, Aalborg University, Frederik Bajers Vej 7H, DK-9220, Aalborg East, Denmark. *****Corresponding authors. E-mail addresses: jakob.diget@jotun.no (J.S. Diget), ttn@bio.aau.dk (T.T. Nielsen)

ARTICLE INFO

Article history: submitted for review 9 November 2018. Revised manuscript submitted 13 February 2019.

Keywords: sulfobetaine, cyclodextrin, click chemistry, ATRP, functional polymers, UCST

ABSTRACT

A versatile atom transfer radical polymerization (ATRP) protocol was developed for the direct homo- and copolymerization of a sulfobetaine monomer, [2-(methacryloyloxy)ethyl]dimethyl-(3-sulfopropyl)ammonium (SBMA), and a mono-functionalized β-cyclodextrin (βCD) methacrylate monomer. The polymers were characterized using 1- and 2D NMR spectroscopy and asymmetrical flow field-flow fractionation (AF4). Low dispersities ($Đ_M = M_w/M_n$) and high initiator efficiencies, of both the homo- and copolymers, indicated good control over the polymerization. The work thus represent one of the few reports where low $Đ_M$ values are obtained for direct ATRP of SBMA and βCD monomers. The novel βCD copolymer showed salt-dependent upper critical solution temperature (UCST) behavior, while isothermal titration calorimetry revealed excellent binding properties.

Introduction

Functional antifouling and antimicrobial polymers are highly relevant within a wide range of research fields, including marine coatings, membrane technology and biomedicine. Poly(ethylene glycol) (PEG) is presumable the most popular antifouling polymer, and functions by hindering adsorption of biomolecules through steric effects and strong repulsive hydration forces [1].

Zwitterionic polymers have recently been highlighted as a favorable alternative to PEG [2-4]. Owing to their charges, the water molecules are more tightly bound, thus resulting in stronger repulsive hydration forces than exerted by PEG [5-7]. The sulfobetaine polymer, poly([2-(methacryloyloxy)ethyl]dimethyl-(3-sulfopropyl)ammonium) (pSBMA), has attracted considerable attention, not only owing to its excellent antifouling properties, but also as it displays upper critical solution temperature (UCST) behavior in aqueous media [8-10]. Homopolymers of SBMA are mainly used for surface coatings, whereas copolymers have a broader range of application and may further improve properties. For instance, SBMA copolymers have been applied as protective corona for micellar structures constructed for drug delivery [11], for the development of temperature responsive micelles [12, 13], as well as improving the antifouling properties [14, 15] and stability of coatings [16].

β-cyclodextrin (βCD) has been studied in similar research areas as antifouling polymers, owing to its capability of encapsulating hydrophobic moieties. This unique feature has for instance been employed for controlled release [17-19], and to construct hierarchical (nano)-structures in both solution [20, 21] and on surfaces [22, 23].

Not surprisingly, antifouling polymers and βCD have been combined previously [24-29] and recently, Zhang et al. reported the synthesis of a PEG-*block*-polyβCD copolymer [21] via the reversible-deactivation radical polymerization (RDRP), atom transfer radical polymerization (ATRP). Though RDRPs offer advantages such as low molar mass distributions ($Đ_M = M_w/M_n$) and controllable molar masses, only this single example of βCD polymers successfully obtained via direct RDRP of βCD monomers, has been reported. pSBMA on the other hand, is often synthesized using RDRP. Reversible addition-fragmentation chain transfer (RAFT) polymerization is often used to directly polymerize SBMA [13, 30-32], whereas group transfer polymerization (GTP) has been carried out on a reactive monomer followed by post-modification to obtain pSBMA [33, 34]. ATRP and surface-initiated ATRP (SI-ATRP) are also frequently used for the direct polymerization of SBMA [35-42]. From the reports where $Đ_M$ values are measured for polymers obtained via direct (SI-) ATRP of SBMA, however, it appears that they increase with molar mass [38-41]. A possible explanation is the poor solubility of the growing chain in H_2O:MeOH (most frequently used solvent). For the single example where low $Đ_M$ values at high molar masses have been reported, a polar solvent (2,2,2-trifluoroethanol) with ions (1-alkyl-3-methylimidazolium chloride) was used [43]. However, a very recent study by Laschewsky and coworkers [42], shows that control is questioned also with this solvent.

It is well known that properties of polymers, and hierarchical structures created thereof, are highly dependent on the molar mass, and thus also $Đ_M$ [44]. As ATRP is already being used broadly for the direct polymerization of SBMA, it is desirable with ATRP protocols that offer control over molar mass and $Đ_M$. Furthermore, it would be highly attractive to combine the properties of pSBMA with those of βCD in linear polymers.

In the current work, we present an ATRP protocol for the direct homo- and copolymerization of SBMA, and a mono-functionalized βCD monomer (PMβCD). The latter was synthesized via "click" chemistry between propargyl methacrylate (PM) and mono-6-azido-6-deoxy-β-cyclodextrin (N_3βCD). Solvent composition was chosen to facilitate solubilization of the monomers and propagating polymers, and the catalytic system was tuned to minimize side-reactions in the polar protic solvent. The novel copolymers, p(SBMA-*co*-

PMβCD), were probed with respect to host-guest interactions and the solution behavior was assessed. The ATRP protocol is of strong interest as it allows direct polymerization of SBMA via ATRP, while low $Đ_M$ values are obtained, and time-consuming post-modification avoided. The novel host-copolymers are highly relevant for the creation of nano-structures or multi-functional surfaces, which is of great interest within, e.g., biomedical sciences or surface and coatings technology.

Experimental

Materials

Acetone (VWR, Haasrode, Belgium), ammonia solution 25% (Merck, Darmstadt, Germany), β-cyclodextrin (Cavamax W7 Pharma, Wacker Chemie, Waterfield, United Kingdom), dimethyl sulfoxide (Fischer Scientific, Loughborough, United Kingdom), pyridine (Fischer Scientific, Loughborough, United Kingdom), Ambersep GT74 (Supelco, Bellefonte, USA), copper powder <63 µm 99.7% (Merck, Darmstadt, Germany), N,N-dimethylformamide puriss >99.8%, ethyl acetate, 2-propanol puriss, diethyl ether >99.9%, dichloromethane ≥99.8%, tetrakis-(acetonitrile)copper(I) hexafluorophosphate, 2,2'-bipyridyl >99%, copper(I)bromide >98%, copper(II)bromide 99%, ethyl 2-bromoisobutyrate 98%, [2-(methacryloyloxy)ethyl]dimethyl-(3-sulfopropyl)ammonium hydroxide 97%, propargyl alcohol 99%, methacryloyl chloride 97%, triethylamine >99%, (+)-sodium L-ascorbate ≥98% (all from Aldrich, Steinheim, Germany). N_3βCD was prepared according to Nielsen et al. [45]. Tris((1-benzyl-1,2,3-triazol-4-yl)methyl)amine (TBTA) was prepared according to Chan et al. [46].

Instrumentation

1- and 2D NMR spectra were recorded on a Bruker DRX600 spectrometer (5 mm TXI (H/C/N) xyz-gradient probe) in $CDCl_3$, DMSO-d_6 or D_2O (Euriso top, Gif-sur-Yvette, France) at 298, 305 and 310 K, respectively. Spectra were calibrated according to the residual solvent signal. The shift of the water signal was calibrated by a temperature dependent formula [47]. ^{1}H- and ^{13}C NMR signals are reported using the indicators shown in figure 1 and 2, for PMβCD and the polymers, respectively. Matrix-assisted laser desorption/ionization-time-of-flight mass spectrometry (MALDI-TOF MS) was carried out on the βCD derivatives with a Bruker Reflex III spectrometer using a double layer matrix of fast evaporating nitro-cellulose and saturated α-cyano-4-hydroxycinnamic acid. Attenuated total reflectance Fourier transform infrared (ATR-FTIR) spectroscopy was carried out on a Varian 660 spectrometer. Dialysis was carried out using MWCO 500 15 mm diameter and MWCO 3500 29 mm diameter from Spectrum Spectra/Por, while freeze-drying was carried out on a Christ Alpha 1-2 LD plus. Thin-layer chromatography (TLC) was used to monitor the synthesis of PM and PMβCD. For the former, it was carried out with an eluent of hexane and ethyl acetate in the ratio of 1:1 by volume. Visualization was made by means of UV light and subsequent Hanessian's stain. For PMβCD an eluent of 2-propanol, water, ethyl acetate and ammonia (5:3:1:1 by volume) was used and visualization was made by UV light, and spraying with 5 vol.% sulfuric acid in ethanol and subsequent heating to 130 °C. Asymmetrical flow field-flow fractionation (AF4) analysis was carried out on an AF2000 FOCUS system (Postnova Analytics, Landsberg, Germany) equipped with a refractive index (RI) detector (PN3140, Postnova) and a multi-angle (seven detectors in the range 35°−145°) light scattering detector (PN3070, λ = 635 nm, Postnova). An aqueous eluent of 0.1 M NaCl with 0.2 g L^{-1} NaN_3 was used. The flow channel was installed with a 350 µm spacer and a regenerated cellulose membrane with a cutoff of 1 or 10 kDa (Z-MEM-AQU-425N, Postnova) depending on molar mass. Data analysis was carried out using the Postnova software (AF2000 Control, version 1.1.025). Values of weight average molar mass (M_w) of the samples in dilute solutions were determined using the Zimm-type fit. Details on the flow setup can be found in the ESI.

The inclusion complexation properties of the p(SBMA-*co*-PMβCD)s were assessed via isothermal titration calorimetry (ITC) and steady-state fluorescence spectroscopy using the fluorescent probe 2-anilinonaphthalene-6-sulfonic acid (2,6-ANS) as guest molecule. ITC measurements were conducted on a MicroCal Auto-ITC 200. 50 and 25 mg mL^{-1} solutions of p(SBMA-*co*-PMβCD)_1 and 2, respectively, corresponding to ~4 mM βCD for both polymers, were prepared in phosphate buffered saline (PBS) and titrated into 201.9 µL PBS or 2,6-ANS (168 µM in PBS) using 20 injections of 2 µL (after an initial injection of 0.4 µL) with 120 s spacing at 25 °C and a stirring speed of 1000 rpm. Data was analyzed in Microcal PEAQ Analysis Software (v.1.0.0.1259) using the "one set of sites" model with "polymer in buffer" and "PBS in 2,6-ANS" subtracted (line) as control. Steady-state fluorescence spectroscopy measurements were conducted on the ITC samples after end titration using a Varian Cary Eclipse fluorescence spectrophotometer.

The solution properties of the polymers were investigated using dynamic light scattering (DLS) analysis and transmittance. DLS measurements were carried out on a Zeta Sizer 3000H from Malvern Instruments, Inc., (He-Ne laser, wavelength of 633 nm and detector angle of 173°). The polymers were solubilized in Milli-Q water (4, 8 and 12 mg mL^{-1}) above their transition temperature and vortexed. The solutions were then cooled slowly to RT and analysed using DLS. Transmittance was recorded on the polymers (6 mg mL^{-1}) in Milli-Q water as a function of temperature from 5 to 70 °C with measurements after each 5 °C increment. Measurements were carried out on a Genesys 10S UV-VIS (500 nm) spectrophotometer (Thermo Scientific) equipped with an external temperature controller.

Synthesis of PMβCD

The synthesis of PMβCD is depicted in scheme 1. PM was synthesized according to the procedure reported by Geng et al., [48], cf. ESI. N_3βCD (5.05 g, 4.35 mmol), TBTA (105 mg, 0.188 mmol) and $Cu(CH_3CN)_4PF_6$ (65 mg, 0.174 mmol) were dissolved in 100 mL degassed DMF. PM (0.675 g, 5.44 mmol) was added directly to the reaction mixture. The reaction was

stirred under inert atmosphere at room temperature (RT). After 24 hrs, TLC indicated complete conversion. The product was precipitated in acetone, filtered, washed with acetone and dried. To remove residues of copper, a solution of the product in a minimum amount of DMSO was swirled over 4 g of Amberlite GT74 resin overnight. The solution was filtered, and the filtrate was dialyzed (MWCO 500 Da) against deionized water for 72 hrs and freeze-dried. The product was isolated as a white fluffy powder (5.12 g, 3.99 mmol, 92% yield). PM: R_f = 0.64. ^{1}H NMR ($CDCl_3$, 600 MHz): δ_H (ppm): 6.17 (d, 1H); 5.62 (d, 1H); 4.75 (d, 2H); 2.47 (m, 1H); 1.96 (s, 3H). PMβCD: R_f = 0.42. ^{1}H NMR (DMSO-d_6, 600 MHz): δ_H (ppm): 8.09 (s, 1H, H^7); 6.03 (s, 1H, H^9); 5.86-5.55 (br, 15H, H^{2c}, H^{3c} and H^9 at 5.68 ppm, overlap); 5.19 (s, 2H, H^8); 5.04-4.75 (br, 7H, H^1); 4.85 and 4.57 (br, 2H, H^{6a}); 4.49-4.4 (br, 5H, H^{6c}); 4.2 (br, 1H, H^{6d}); 4.0 (br, 1H, H^{5a}); 3.8-3.48 (br, 23H, H^3, H^5 and H^6 overlap); 3.43-3.3 (br, 7H, H^4, overlap with HDO); 3.4-3.23 (br, 7H, H^2, overlap with HDO); 3.07 and 2.875 (br, 2H, H^{6b}); 1.88 (s, 3H, H^{10}): ^{13}C NMR (DMSO-d_6, 600 MHz): δ_C (ppm): 126.5 (1C, C^9); 126 (1C, C^7); 102.5 (7C, C^1); 84.2-81.3 (7C, C^4); 74-72 (13C, C^3 and C^5 overlap); 72.9 (7C, C^2); 70.4 (1C, C^{5a}); 60.4 (5C, C^6); 59.5 (1C, C^{6b}); 58.1 (1C, C^8); 50.85 (1C, C^{6a}); 18.5 (1C, C^{10}). MALDI-TOF MS: m/z 1306.6 [PMβCD+Na^+].

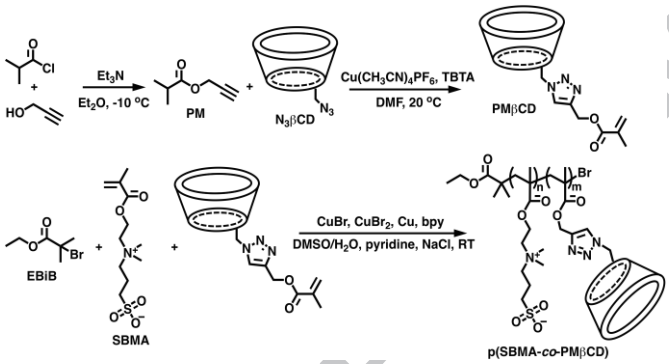

Scheme 1. Synthesis schematics; PMβCD (top) and polymer synthesis with p(SBMA-*co*-PMβCD) as example (bottom).

Synthesis of polymers

Synthesis of p(SBMA-*co*-PMβCD)_2 using ATRP is depicted in scheme 1 and explained below. Similar approaches were used for the other ATRPs. An overview of the detailed synthesis conditions can be found in table S1.

SBMA (0.553 g, 1.979 mmol) and PMβCD (0.459 g, 0.358 mmol) were dissolved in a solvent mixture of 12 mL DMSO:pyridine:0.85 M NaCl saline water (69:6:25 vol.%) in a Florence flask. The solution was purged with nitrogen under stirring for 15 min. The atmosphere of the reaction vessel was evacuated under reduced pressure and replaced with nitrogen, purged with nitrogen for 5 min and sonicated for 20 min. The solution was then further deaerated with nitrogen for 5 min and placed under reduced pressure for 5 min, which was repeated two more times before sealing the vessel under argon atmosphere.

Another Florence flask with bpy (14.2 mg, 0.091 mmol), Cu(0) (19.9 mg, 0.0313 mmol), CuBr (4.5 mg, 0.0313 mmol) and $CuBr_2$ (1.57 mg, 0.0069 mmol) was flushed with nitrogen for 5 min and evacuated for 5 min three times before sealed under argon atmosphere. A Hamilton syringe was flushed with argon and used to add the monomer solution to the flask containing the catalytic system. The solution was bubbled 3 min with argon. Finally, ethyl 2-bromoisobutyrate (EBiB) (3.8 µL, 0.026 mmol) was added and the flask was sealed under argon atmosphere and placed in an oil bath for 24 hrs under stirring at 30 °C. The reaction was stopped by subjecting it to normal atmosphere, indicated by a color change from brown to green or blue. The solution was dialyzed (MWCO 3500 Da) against 0.1 M NaCl (aq) for 48 hrs and deionized water for 48 hrs and freeze-dried (0.461 g, 45.5%). p(SBMA-*co*-PMβCD): ^{1}H NMR (D_2O, 600 MHz): δ_H (ppm): 8.18 (s, 1H, H^7); 5.3-4.9 (br, 10H, H^1, H^{6a} at 4.99 ppm and H^8 at 5.24 ppm, overlap); 4.79 (s, 1H, H^{6a}); 4.53 (br, 2H, H^a); 4.16-4.12 (br, 3H, H^{5a} and H^B); 4.05-3.73 (br, 25H, H^3, H^5 ,H^6 and H^b, overlap); 3.73-3.5 (br, 16H, H^2, H^4 and H^d, overlap); 3.31 and 3.1 (br, 2H, H^{6b}); 3.25 (br, 6H, H^c); 3.0 (br, 2H, H^f); 2.3 (br, 2H, H^e); 2.18-1.65 (br, 2H, H^D); 1.4-0.3 (br, 12H, H^A, H^C and H^E): ^{13}C NMR (D_2O, 600 MHz): δ_C (ppm) βCD: 128 (1C, C^7); 102 (7C, C^1); 82.5-71.5 (14C, C^2 and C^4 overlap); 73.9-71.3 (13C, C^3 and C^5 overlap); 70.3 (1C, C^{5a}); 63.5 (1C, C^d); 62.3 (1C, C^b); 62.2 (1C, C^B); 60.5 (5C, C^6); 59.7 and 59.4 (1C, C^{6b}); 59.3 (1C, C^a); 57.7 (1C, C^8); 56.2 (1C, C^D); 51.6 (1C, C^c); 51.15 and 50.97 (1C, C^{6a}); 47.6 (1C, C^f); 18.6 (1C, C^e); 21.3-17.2 (3C, C^C and C^E); 13.5 (1C, C^A). Cf. ESI for chemical shifts of the homopolymers.

Results and Discussion

Synthesis of PMβCD

Synthesis of PMβCD has previously been reported using CuAAC by *in situ* reduction of $CuSO_4$ with NaAsc at either 140 °C, RT or microwave-assisted at RT [49]. At 140 °C the yield was limited to 57% and the product was a mixture of 1,4-and 1,5-adducts. At RT the 1,4-adducts were favoured and yields of 84% and 74% were obtained with and without microwaves, respectively. However, the latter required one week for completion of the reaction. In the current study, CuAAC was carried out using a catalytic system of $Cu(CH_3CN)_4PF_6$, TBTA and NaAsc. The reaction was carried out at RT overnight and resulted in an excellent yield of 92% exclusively constituting the 1,4-adduct. From ^{1}H NMR analysis, the appearance of a triazol proton signal at 8.09 ppm clearly reveals the successful CuAAC. A splitting of the signal is observed, but has previously been ascribed to self-inclusion, where the triazol proton signals upfield belongs to the cyclodextrin derivatives for which self-inclusion occurs [50]. Previously, the two vinyl group protons of PMβCD have been assigned to the signals at 5.19 and 6.07 ppm [49], but from COSY- and HSQC NMR it is evident that the vinyl group protons reside at 5.68 and 6.03-6.07 ppm. A complete signal assignment can be found in the HSQC spectrum in figure 1. MALDI-TOF MS analysis and the ratio of the ^{1}H NMR integral of the triazol proton to those of

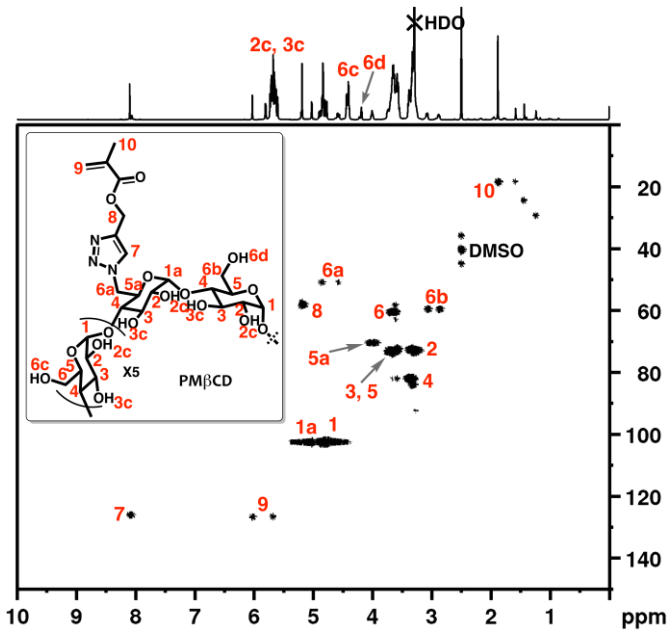

Figure 1 – HSQC NMR spectrum of PMβCD in DMSO-d_6 at 305 K with assignment of signals.

the protons from βCD and PM, supports that mono-substituted PMβCD has been synthesized. NMR- and MALDI-TOF MS spectra can be found in the ESI.

Polymerization

pSBMA, pPMβCD and p(SBMA-*co*-PMβCD) were successfully synthesized using ATRP. High initiator efficiencies and low $Đ_M$ values were obtained, thus supporting controlled polymerization, cf. table 1.

NMR was used to assess the chemical structure and determine M_n values via end-group analysis (cf. ESI for details). AF4, for which separation of analytes occur solely through the interaction of the analyte with an external physical eluent field, rather than by interaction with a stationary phase, was used to determine the M_w- and $Đ_M$ values. Cf. figure 2 and 3 for ^{1}H NMR spectra, including assignment of signals, and AF4 molar mass distribution plots, respectively. For ^{1}H NMR of the copolymers, the signals reside at same shifts as for the homopolymers, where the SBMA signals H^b and H^d overlap with the βCD signals H^3, H^5 and H^6, and H^2 and H^4, respectively.

pPMβCD was synthesized in 1 M pyridine in DMSO (pyridine:DMSO, 8:92 vol.%). The M_w corresponds to a degree of polymerization (DP) of approx. 10, which is significantly lower than the targeted DP of 25 – however, it corresponds with values reported independently by other groups [21, 49, 51], and indicates an upper limit for the DP of βCD monomers with a relatively short linker between the methacrylate and βCD. Homogeneous polymerization conditions and low $Đ_M$ values were achieved in a solvent mixture of DMSO, pyridine and NaCl saline water for pSBMA and the copolymers, whereas heterogeneous polymerization conditions and large $Đ_M$ values were obtained in DMSO and DMSO:H_2O without NaCl (varying solvent volumes and ratios, cf. table S1 and S2). Early attempts using MeOH:H_2O (1:1 wt., without salt), were unsuccessful as PMβCD was poorly soluble in this solvent, and polymerization of SBMA led to heterogenous reaction conditions as the ATRP progressed. The latter was surprising at first as the many ATRPs of SBMA (i.e., not post modification method) are carried out in MeOH:H_2O. However, most of the reported ATRPs are in fact SI-ATRPs, making it difficult to measure $Đ_M$ values and to see the heterogenous reaction conditions. The few examples where $Đ_M$ values have in fact been measured, they seemingly increase with increasing M_w [38-41]. Moreover, Terayama et al., carried out SI-ATRP and normal ATRP simultaneously in MeOH:H_2O (without salt) [43]. Heterogeneous reaction conditions were observed, and large $Đ_M$ values were obtained for both the polymer synthesized in solution, and the one cleaved from the surface. As in the presented study, where pSBMA was synthesized with a low $Đ_M$ of 1.14 at a relatively large M_w of 30.5 kg mol^{-1}, Terayama et al., obtained homogenous reaction conditions and low $Đ_M$ values with a polar solvent (2,2,2-trifluoroethanol) in the presence of ions (1-alkyl-3-methylimidazolium chloride) [43]. As polar protic solvents and ions tend to increase side-reactions, we added pyridine (pyr) as helper-ligand or co-solvent to suppress Cu(I) disproportionation reactions [52-54]. Cu(0) was added as activator- and reducing agent, thus resulting in supplemental activator and reducing agent (SARA) ATRP. Though it is hypothesized that RDRP carried out in the presence of Cu(0) may also result in single electron transfer living radical polymerization (SET-LRP), it is found, in the review article of Matyjaszewski and co-workers [55], that the available literature on RDRP carried out in the presence of Cu(0) agree with the SARA ATRP mechanism rather than the SET-LRP. SARA ATRP occurs if Cu(I) is the main activator,

Table 1 – AF4- and ^{1}H NMR analysis. All molar masses are given in kg mol^{-1}.

Name and structure[a]	$M_{(aim)}$[b]	$M_{w(AF4)}$	$Đ_{M(AF4)}$	$M_{n(NMR)}$[a]	% mole βCD	% yield	Initiator efficiency [%][c]
pSBMA_6_{88}[d]	35	30.5	1.14	24.8±0.2	N/A	60	84
pPMβCD$_{10.5}$[e]	32	12.4	1.14	13.9±0.2	100	42	95
p(SBMA$_{46}$-*co*-PMβCD$_{1.6}$)_1[e]	17.5	16.5	1.28	15±0.2	3.35	64	74
p(SBMA$_{55}$-*co*-PMβCD$_{4.5}$)_2[e]	39	24.6	1.17	21.4±0.2	7.5	46	82

[a]M_n and repeating units calculated using ^{1}H NMR end-group analysis as explained in the ESI. Number of repeating units is indicated in subscript in the first column. [b]Calculated from added amounts of initiator and monomer during synthesis. [c]Calculated from the $M_{n(NMR)}$ values and isolated masses as follows: ((Isolated mass) / $M_{n(NMR)}$) / (moles of EBiB). [d]10- and [e]1 kDa cutoff separation membrane used for the AF4 analysis.

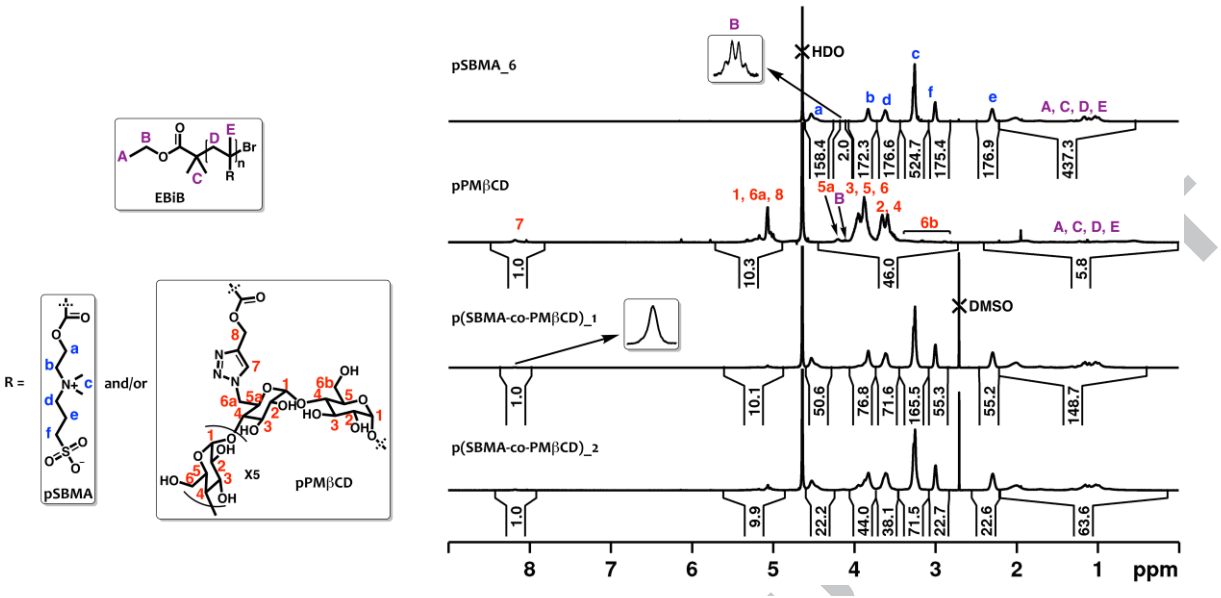

Figure 2 – ^{1}H NMR spectra of the polymers in 0.1 M NaCl (D_2O) at 310 K with assignment of signals.

which is the case if disproportionation is minimal. In the current work, pyridine was added to suppress disproportionation and the presence of Cu(I) was clearly indicated from the brown color of the reaction medium. Moreover, in the above-mentioned review, it is highlighted that RDRP in presence of Cu(0) carried out in H_2O and DMSO follows the SARA ATRP mechanism. $CuBr_2$ was added to suppress initial termination [56], and has been reported to significantly improve the control of reaction in conjunction with Cu(0) [57] and for ATRP carried out in polar protic solvents, as reversible dissociation of halides and sub-sequential coordination of the Cu(II) species are more pronounced in polar (protic) solvents; hence resulting in inefficient deactivation [53]. With these conditions, the ATRP system remained active throughout the synthesis and high initiator efficiencies were obtained.

Typical initiator efficiencies are in the range of 50-80% [58], whereas we obtained 74-95%. The lower initiator efficiencies

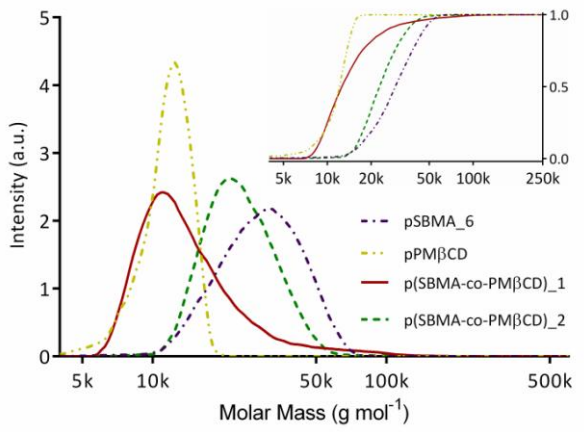

Figure 3 – Differential and cumulative (insert) molar mass distribution of the polymers obtained using AF4 analysis.

of the pSBMA and p(SBMA-*co*-PMβCD)s relative to that of the pPMβCD (74-84% and 95%, respectively) may be explained by the solvent differences where that of p(SBMA-*co*-PMβCD) contains H_2O, thus favouring Cu(II) species, which in turn results in a higher concentration of radicals, and therefore a higher degree of early initiator termination. The slightly larger $Đ_M$ value obtained for p(SBMA-*co*-PMβCD)_1 (1.28 vs. 1.17) is probably a coincident as there was no difference in ATRP conditions and since homopolymerization, under similar conditions, resulted in pPMβCD and pSBMA_6 both with low $Đ_M$ values of 1.14. The amount of incorporated βCD could be controlled, though slightly less than 50% of the theoretical amount of PMβCD was incorporated – most likely because of differences in reactivity and bulkiness of the monomers, thus also indicating a gradient-like structure. 3.35 and 7.5 mole % βCD were incorporated for p(SBMA-*co*-PMβCD)_1 and 2, respectively.

Evaluation of βCD host-guest inclusion complexation

Host-guest abilities of p(SMBA-*co*-PMβCD)_1 and 2 in aqueous solution were assessed via ITC and steady-state fluorescence spectroscopy using the fluorescent probe 2,6-ANS as βCD guest molecule. In water, 2,6-ANS displays only weak fluorescence, primarily ascribed to efficient quenching by dipolar water molecules. Upon inclusion in the hydrophobic βCD cavity, however, the fluorescence intensity (FI) increases accompanied by a blue shift of emission maximum in response to the change in polarity, i.e. shielding from aqueous solution [59, 60]. The integrated ITC heat plots for titration of p(SMBA-*co*-PMβCD)_1 and 2 into 2,6-ANS (figure 4), confirms the expected 1:1 stoichiometry for the binding mode, while the corresponding titration with pSBMA_6 (cf. S22) yields limited interaction. The derived association constant of 4386 M^{-1} and 4545 M^{-1} for p(SMBA-*co*-PMβCD)_1 and 2, respectively, is notably higher than that previously reported on parent βCD (2550 M^{-1}) [61]. The stronger affinity can be ascribed to the

presence of the linker on the primary face of βCD, essentially extending the hydrophobic βCD cavity, and interactions with the polymer backbone. This is further substantiated by the emission spectra acquired on the ITC samples after the titration (figure 5). For both polymer samples, a strong enhancement of the FI is observed, as compared to pSMBA_6 and 2,6-ANS alone, with p(SMBA-*co*-PMβCD)_2 yielding a slightly higher FI than p(SMBA-*co*-PMβCD)_1. While the FI is sensitive to changes in host concentration, i.e. number of formed complexes, the blue-shift of the emission maximum (EM) is a direct measure of the polarity of the local environment experienced by 2,6-ANS. For both polymer samples the EM of 2,6-ANS is shifted from 475 nm to 433 nm, while the value for parent βCD/2,6-ANS is 450 nm [61]. In this context it should be noted that the dimensions of 2,6-ANS exceeds the dimensions of the βCD cavity. Consequently, the significant shift in EM indicates that the 2,6-ANS moiety, normally protruding from the βCD cavity, is efficiently shielded from the solvent upon inclusion complexation with the polymers. The minor FI enhancement and blue-shift of the EM observed for pSBMA_6 may indicate that, in the abscense of βCD cavities, the poorly soluble 2,6-ANS stacks in-between the hydrophobic segments of the homo-polymer.

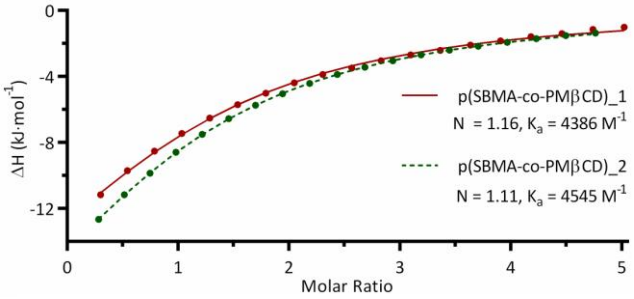

Figure 4 – Enthalpograms for the titration of p(SBMA-*co*-PMβCD)_1 and 2 with 2,6-ANS.

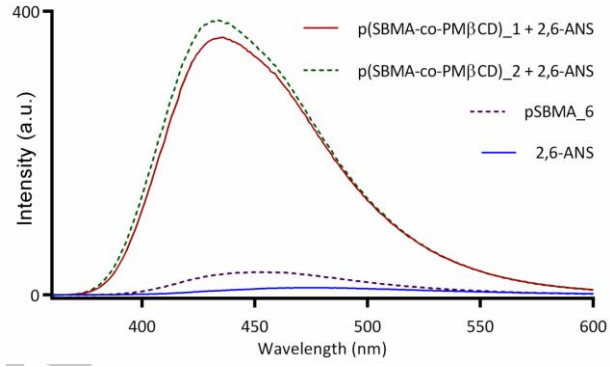

Figure 5 – Fluorescence emission spectra of 2,6-ANS (~150 μM) with and without pSBMA_6 (10 mg mL^{-1}), p(SBMA-*co*-PMβCD)_1 (10 mg mL^{-1}) and 2 (5 mg mL^{-1}).

UCST behavior

It is well-documented that the thermo-responsive behavior of pSBMA depends on molar mass and concentration and that the intra- and inter molecular bonds break in the presence of salt whereby solubility is promoted [8, 9, 62]. These properties have been used to synthesize salt- and temperature responsive pSBMA based nanoparticles [12, 13].

In the current work, the solution behavior of the pPMβCD, pSBMA_1-6 (cf. table S2 for details) and p(SBMA-*co*-PMβCD)_1 and 2 was assessed. The polymers were dissolved above their phase transition temperature and allowed to cool to RT for agglomeration. pSBMA_3-5 (M_w > 77 kg mol^{-1}) displayed the typical UCST response and dissolved at elevated temperatures whereas they precipitated during cooling to RT. Addition of NaCl resulted in complete dissolution at RT. pSBMA_1 and 6 (M_w = 8 and 30.5 kg mol^{-1}, respectively) were soluble in aqueous solution at RT. In a recent study [62] however, cloud points for pSBMA with 85 repeating units (M_n of 26-31 kg mol^{-1}), and presumably low $Đ_M$ values, were determined to 28-35 ^{o}C for 4-12 mg mL^{-1}. The discrepancy in solution behavior may possibly be explained by the presence of some residual salt in the pSBMA of the current study, as they were purified by dialysis against salt water followed by deionized water (replaced continuously). It is well known that even small amounts of salt contaminants will decrease the cloud point of pSBMA. In the aforementioned study [62], it was sought to avoid contaminating salt.

pPMβCD and the copolymer with the highest βCD content, p(SBMA-*co*-PMβCD)_2 containing 25.6% wt. PMβCD repeating units, were completely soluble in aqueous solution at RT. As opposed to this, p(SBMA-*co*-PMβCD)_1, with 12.8% wt. PMβCD repeating units, was insoluble in deionized water at RT, whereas it dissolved at elevated temperatures. Upon cooling to RT, particle sizes of 260, 370, and 400 nm were obtained for solutions of 4, 8 and 12 mg mL^{-1}, respectively (cf. figures S23-25 for DLS data). In all cases, unassociated polymer chains were observed with bimodal size distributions of dissolved polymers and aggregates. This indicates either that the aggregation had not yet reached equilibrium, or that only the largest fractions of the polymers were able to form aggregates. The latter might be due to residual salt in the polymers. Heating or addition of salt resulted in complete dissolution of the aggregates, as indicated by the unimodal size distribution of <7.5 nm from DLS. When looking at transmittance as a function of temperature, indication of a UCST type behavior of the polymer can be seen (cf. figure S26), albeit a rather weak DLS response was observed. However, the weak signal can be explained by the before-mentioned bimodal distribution or presence of residual salt in the polymer. The results reveal that p(SBMA-*co*-PMβCD) shows UCST type behavior, which is dependent on the content of βCD. This is expected, as the presence of the βCD-moieties impedes the electrostatic interactions between the SMBA-moieties. As the main focus of the present work is on the development of a versatile ATRP-protocol for the (co-) polymerization of SBMA, further elucidation of the UCST behavior was considered out of scope. Previously, UCST type behavior has been indicated for βCD-containing polyelectrolytes [63, 64]. In both examples, an inclusion complex with a guest molecule of opposite charge was formed to provoke the UCST behavior. In the case of p(SBMA-*co*-PMβCD)_1 however, the polymer itself shows UCST behavior, while the βCD cavities are left readily accessible.

Conclusion

Mono-substituted PMβCD was synthesized with an excellent yield via the CuAAC reaction, and an ATRP protocol was developed for the direct homo- and copolymerization of PMβCD and SBMA. Low $Đ_M$ values and high initiator efficiencies were obtained. The ATRPs thus represent some of the few successful ATRPs reported for SBMA and βCD monomers. For polymerization of SBMA, solubility proved key in obtaining control and was facilitated using a polar protic solvent (DMSO:H_2O) with salt. The novel copolymer, p(SBMA-*co*-PMβCD), displays salt-dependent UCST behavior, and while more studies are needed, this represents one of the first examples of a βCD polymer displaying UCST behavior. Further, ITC and steady-state fluorescence spectroscopy confirmed the accessibility of the βCD cavities, and thereby that the copolymers exhibit the unique feature of inclusion complex formation.

The novel copolymers have potential within a range of applications, for instance; biosensors, coating technology, and drug delivery, while the developed synthesis protocols ease the synthesis of new SBMA and βCD based polymeric materials.

An obvious continuation of this study would be to apply this novel protocol to synthesize pSBMA and p(SBMA-*co*-PMβCD) with higher M_w and further investigate the UCST behavior of these copolymers. Polymerization kinetics should be investigated to elucidate the nature of the reaction and improve the protocol. This could be achieved by e.g., quenching the reaction at 85-90 % monomer conversion, thus limiting termination and side reactions while obtaining a high conversion.

Appendix A. Supplementary material

Supplementary data associated with this article can be found, in the online version, at http://dx.doi.org/XX

Acknowledgements

JSD greatly appreciate the financial support of the European Commission through the NanoS3 project (Grant No. 290251) of the FP7-PEOPLE-2011-ITN call.

References

[1] P. Harder, M. Grunze, R. Dahint, G. Whitesides, P. Laibinis, Molecular conformation in oligo (ethylene glycol)-terminated self-assembled monolayers on gold and silver surfaces determines their ability to resist protein adsorption, The Journal of Physical Chemistry B 102(2) (1998) 426-436.
[2] S. Liu, S. Jiang, Chemical conjugation of zwitterionic polymers protects immunogenic enzyme and preserves bioactivity without polymer-specific antibody response, Nano Today 11(3) (2016) 285-291.
[3] A.S. Hoffman, The early days of PEG and PEGylation (1970s–1990s), Acta Biomaterialia 40 (2016) 1-5.
[4] P. Zhang, F. Sun, S. Liu, S. Jiang, Anti-PEG antibodies in the clinic: Current issues and beyond PEGylation, Journal of Controlled Release 244 (2016) 184-193.
[5] S. Chen, J. Zheng, L. Li, S. Jiang, Strong resistance of phosphorylcholine self-assembled monolayers to protein adsorption: insights into nonfouling properties of zwitterionic materials, Journal of the American Chemical Society 127(41) (2005) 14473-14478.
[6] Y. He, J. Hower, S. Chen, M.T. Bernards, Y. Chang, S. Jiang, Molecular simulation studies of protein interactions with zwitterionic phosphorylcholine self-assembled monolayers in the presence of water, Langmuir 24(18) (2008) 10358-10364.
[7] J. Wu, W. Lin, Z. Wang, S. Chen, Y. Chang, Investigation of the hydration of nonfouling material poly (sulfobetaine methacrylate) by low-field nuclear magnetic resonance, Langmuir 28(19) (2012) 7436-7441.
[8] V.M. Soto, J. Galin, Poly (sulphopropylbetaines): 2. Dilute solution properties, Polymer 25(2) (1984) 254-262.
[9] D. Schulz, D. Peiffer, P. Agarwal, J. Larabee, J. Kaladas, L. Soni, B. Handwerker, R. Garner, Phase behaviour and solution properties of sulphobetaine polymers, Polymer 27(11) (1986) 1734-1742.
[10] M.B. Huglin, M.A. Radwan, Properties of poly [N-2-(methyacryloyloxy) ethyl-N, N-dimethyl-N-3-sulfopropylammonium betaine] in dilute solution, Die Makromolekulare Chemie 192(10) (1991) 2433-2445.
[11] S. Zhai, Y. Ma, Y. Chen, D. Li, J. Cao, Y. Liu, M. Cai, X. Xie, Y. Chen, X. Luo, Synthesis of an amphiphilic block copolymer containing zwitterionic sulfobetaine as a novel pH-sensitive drug carrier, Polymer Chemistry 5(4) (2014) 1285-1297.
[12] J. Weaver, S. Armes, V. Bütün, Synthesis and aqueous solution properties of a well-defined thermo-responsive schizophrenic diblock copolymer, Chemical Communications (18) (2002) 2122-2123.
[13] K.E. Doncom, H. Willcock, R.K. O'Reilly, The direct synthesis of sulfobetaine-containing amphiphilic block copolymers and their self-assembly behavior, European Polymer Journal 87 (2017) 497-507.
[14] W.H. Kuo, M.J. Wang, H.W. Chien, T.C. Wei, C. Lee, W.B. Tsai, Surface modification with poly(sulfobetaine methacrylate-co-acrylic acid) to reduce fibrinogen adsorption, platelet adhesion, and plasma coagulation, Biomacromolecules 12(12) (2011) 4348-56.
[15] J.-H. Li, M.-Z. Li, J. Miao, J.-B. Wang, X.-S. Shao, Q.-Q. Zhang, Improved surface property of PVDF membrane with amphiphilic zwitterionic copolymer as membrane additive, Applied Surface Science 258(17) (2012) 6398-6405.
[16] R. Quintana, M. Gosa, D. Jańczewski, E. Kutnyanszky, G.J. Vancso, Enhanced stability of low fouling zwitterionic polymer brushes in seawater with diblock architecture, Langmuir 29(34) (2013) 10859-10867.
[17] N. Zhang, J. Li, W. Jiang, C. Ren, J. Li, J. Xin, K. Li, Effective protection and controlled release of insulin by cationic β-cyclodextrin polymers from alginate/chitosan nanoparticles, International Journal of Pharmaceutics 393(1-2) (2010) 213-219.
[18] F. Hirayama, K. Uekama, Cyclodextrin-based controlled drug release system, Advanced Drug Delivery Reviews 36(1) (1999) 125-141.
[19] M. Kamada, F. Hirayama, K. Udo, H. Yano, H. Arima, K. Uekama, Cyclodextrin conjugate-based controlled release system: repeated-and prolonged-releases of ketoprofen after oral administration in rats, Journal of Controlled Release 82(2-3) (2002) 407-416.
[20] V. Wintgens, T.T. Nielsen, K.L. Larsen, C. Amiel, Size-Controlled Nanoassemblies Based on Cyclodextrin-Modified Dextrans, Macromolecular Bioscience 11(9) (2011) 1254-1263.
[21] M. Zhang, Q. Xiong, W. Shen, Q. Zhang, Facile synthesis of well-defined cyclodextrin-pendant polymer via ATRP for nanostructure fabrication, RSC Advances 4(58) (2014) 30566.
[22] J. Deng, X. Liu, S. Zhang, C. Cheng, C. Nie, C. Zhao, Versatile and Rapid Postfunctionalization from Cyclodextrin Modified Host Polymeric Membrane Substrate, Langmuir 31(35) (2015) 9665-9674.
[23] Z.-Q. Shi, Y.-T. Cai, J. Deng, W.-F. Zhao, C.-S. Zhao, Host–Guest Self-Assembly Toward Reversible Thermoresponsive Switching for Bacteria Killing and Detachment, ACS Applied Materials & Interfaces 8(36) (2016) 23523-23532.
[24] M.E. Davis, Design and development of IT-101, a cyclodextrin-containing polymer conjugate of camptothecin, Advanced Drug Delivery Reviews 61(13) (2009) 1189-1192.
[25] M.E. Davis, M.E. Brewster, Cyclodextrin-based pharmaceutics: past, present and future, Nature Reviews Drug Discovery 3(12) (2004) 1023-1035.
[26] W. Lin, G. Ma, J. Wu, S. Chen, Different in vitro and in vivo behaviors between Poly (carboxybetaine methacrylate) and poly (sulfobetaine methacrylate), Colloids and Surfaces B: Biointerfaces 146 (2016) 888-894.
[27] M. Zhang, W. Shen, Q. Xiong, H. Wang, Z. Zhou, W. Chen, Q. Zhang, Thermo-responsiveness and biocompatibility of star-shaped poly [2-(dimethylamino) ethyl methacrylate]-b-poly (sulfobetaine methacrylate) grafted on a β-cyclodextrin core, RSC Advances 5(36) (2015) 28133-28140.

[28] W. Lin, G. Ma, F. Ji, J. Zhang, L. Wang, H. Sun, S. Chen, Biocompatible long-circulating star carboxybetaine polymers, Journal of Materials Chemistry B 3(3) (2015) 440-448.
[29] Y. Li, H. Guo, J. Zheng, J. Gan, Y. Zhang, X. Guan, K. Wu, M. Lu, Synthesis and encapsulation of an amphiphilic thermoresponsive star polymer with β-cyclodextrin and hyperbranched poly (oligo (ethylene glycol) methacrylate) as building blocks, RSC Advances 4(97) (2014) 54268-54281.
[30] M.S. Donovan, A.B. Lowe, T.A. Sanford, C.L. McCormick, Sulfobetaine-containing diblock and triblock copolymers via reversible addition-fragmentation chain transfer polymerization in aqueous media, Journal of Polymer Science Part A: Polymer Chemistry 41(9) (2003) 1262-1281.
[31] D. Wang, T. Wu, X. Wan, X. Wang, S. Liu, Purely salt-responsive micelle formation and inversion based on a novel schizophrenic sulfobetaine block copolymer: structure and kinetics of micellization, Langmuir 23(23) (2007) 11866-11874.
[32] H. Willcock, A. Lu, C.F. Hansell, E. Chapman, I.R. Collins, R.K. O'Reilly, One-pot synthesis of responsive sulfobetaine nanoparticles by RAFT polymerisation: the effect of branching on the UCST cloud point, Polymer Chemistry 5(3) (2014) 1023-1030.
[33] A.B. Lowe, N.C. Billingham, S.P. Armes, Synthesis of polybetaines with narrow molecular mass distribution and controlled architecture, Chemical Communications (13) (1996) 1555-1556.
[34] A.B. Lowe, N.C. Billingham, S.P. Armes, Synthesis and properties of low-polydispersity poly (sulfopropylbetaine) s and their block copolymers, Macromolecules 32(7) (1999) 2141-2148.
[35] J. Ladd, Z. Zhang, S. Chen, J.C. Hower, S. Jiang, Zwitterionic polymers exhibiting high resistance to nonspecific protein adsorption from human serum and plasma, Biomacromolecules 9(5) (2008) 1357-1361.
[36] Z. Zhang, T. Chao, S. Chen, S. Jiang, Superlow fouling sulfobetaine and carboxybetaine polymers on glass slides, Langmuir 22(24) (2006) 10072-10077.
[37] Z. Zhang, S. Chen, Y. Chang, S. Jiang, Surface grafted sulfobetaine polymers via atom transfer radical polymerization as superlow fouling coatings, The Journal of Physical Chemistry B 110(22) (2006) 10799-10804.
[38] Y. Chang, S. Chen, Z. Zhang, S. Jiang, Highly protein-resistant coatings from well-defined diblock copolymers containing sulfobetaines, Langmuir 22(5) (2006) 2222-2226.
[39] Y.J. Shih, Y. Chang, A. Deratani, D. Quemener, "Schizophrenic" hemocompatible copolymers via switchable thermoresponsive transition of nonionic/zwitterionic block self-assembly in human blood, Biomacromolecules 13(9) (2012) 2849-58.
[40] G. Li, G. Cheng, H. Xue, S. Chen, F. Zhang, S. Jiang, Ultra low fouling zwitterionic polymers with a biomimetic adhesive group, Biomaterials 29(35) (2008) 4592-4597.
[41] H.S. Sundaram, X. Han, A.K. Nowinski, J.-R. Ella-Menye, C. Wimbish, P. Marek, K. Senecal, S. Jiang, One-step dip coating of zwitterionic sulfobetaine polymers on hydrophobic and hydrophilic surfaces, ACS Applied Materials & Interfaces 6(9) (2014) 6664-6671.
[42] N.M. Nizardo, D. Schanzenbach, E. Schönemann, A. Laschewsky, Exploring Poly (ethylene glycol)-Polyzwitterion Diblock Copolymers as Biocompatible Smart Macrosurfactants Featuring UCST-Phase Behavior in Normal Saline Solution, Polymers 10(3) (2018) 325.
[43] Y. Terayama, M. Kikuchi, M. Kobayashi, A. Takahara, Well-defined poly (sulfobetaine) brushes prepared by surface-initiated ATRP using a fluoroalcohol and ionic liquids as the solvents, Macromolecules 44(1) (2010) 104-111.
[44] K.E. Doncom, L.D. Blackman, D.B. Wright, M.I. Gibson, R.K. O'Reilly, Dispersity effects in polymer self-assemblies: a matter of hierarchical control, Chemical Society Reviews 46(14) (2017) 4119-4134.
[45] T.T. Nielsen, V. Wintgens, C. Amiel, R. Wimmer, K.L. Larsen, Facile synthesis of β-cyclodextrin-dextran polymers by "click" chemistry, Biomacromolecules 11(7) (2010) 1710-1715.
[46] T.R. Chan, R. Hilgraf, K.B. Sharpless, V.V. Fokin, Polytriazoles as copper(I)-stabilizing ligands in catalysis, Organic Letters 6(17) (2004) 2853-2855.
[47] H.E. Gottlieb, V. Kotlyar, A. Nudelman, NMR chemical shifts of common laboratory solvents as trace impurities, The Journal of Organic Chemistry 62(21) (1997) 7512-7515.
[48] J. Geng, G. Mantovani, L. Tao, J. Nicolas, G. Chen, R. Wallis, D.A. Mitchell, B.R. Johnson, S.D. Evans, D.M. Haddleton, Site-directed conjugation of "clicked" glycopolymers to form glycoprotein mimics: binding to mammalian lectin and induction of immunological function, Journal of the American Chemical Society 129(49) (2007) 15156-15163.
[49] M. Munteanu, S. Choi, H. Ritter, Cyclodextrin methacrylate via microwave-assisted click reaction, Macromolecules 41(24) (2008) 9619-9623.
[50] J. Potier, S. Menuel, N. Azaroual, E. Monflier, F. Hapiot, Limits of the Inversion Phenomenon in Triazolyl-Substituted β-Cyclodextrin Dimers, European Journal of Organic Chemistry 2014(7) (2014) 1547-1556.
[51] A. Harada, M. Furue, S.-i. Nozakura, Cyclodextrin-containing polymers. 1. Preparation of polymers, Macromolecules 9(5) (1976) 701-704.
[52] N. Tsarevsky, T. Pintauer, K. Matyjaszewski, Atom transfer radical polymerization of ionic monomers in aqueous solution: Mechanistic studies and synthesis, Abstracts of papers of the American Chemical Society, American Chemical Society 1155 16TH ST, NW, Washington, DC 20036 USA, 2002, pp. U440-U440.
[53] N.V. Tsarevsky, T. Pintauer, K. Matyjaszewski, Deactivation efficiency and degree of control over polymerization in ATRP in protic solvents, Macromolecules 37(26) (2004) 9768-9778.
[54] N.V. Tsarevsky, K. Matyjaszewski, "Green" atom transfer radical polymerization: from process design to preparation of well-defined environmentally friendly polymeric materials, Chemical Reviews 107(6) (2007) 2270-2299.
[55] D. Konkolewicz, Y. Wang, P. Krys, M. Zhong, A.A. Isse, A. Gennaro, K. Matyjaszewski, SARA ATRP or SET-lRP. end of controversy?, Polymer Chemistry 5(15) (2014) 4396-4417.
[56] K. Matyjaszewski, M. Wei, J. Xia, S.G. Gaynor, Atom transfer radical polymerization of styrene catalyzed by copper carboxylate complexes, Macromolecular Chemistry and Physics 199(10) (1998) 2289-2292.
[57] K. Matyjaszewski, S. Coca, S.G. Gaynor, M. Wei, B.E. Woodworth, Zerovalent metals in controlled/"living" radical polymerization, Macromolecules 30(23) (1997) 7348-7350.
[58] W.A. Braunecker, K. Matyjaszewski, Controlled/living radical polymerization: Features, developments, and perspectives, Progress in Polymer Science 32(1) (2007) 93-146.
[59] E.M. Kosower, H. Dodiuk, H. Kanety, Intramolecular donor-acceptor system. 4. Solvent effects on radiative and nonradiative processes for the charge-transfer states of N-arylaminonaphthalenesulfonates, Journal of the American Chemical Society 100(13) (1978) 4179-4188.
[60] B.D. Wagner, N. Stojanovic, A.I. Day, R.J. Blanch, Host properties of cucurbit [7] uril: fluorescence enhancement of anilinonaphthalene sulfonates, The Journal of Physical Chemistry B 107(39) (2003) 10741-10746.
[61] L.W. Städe, T.T. Nielsen, L. Duroux, R. Wimmer, K. Shimizu, K.L. Larsen, Synthesis and surface grafting of a β-cyclodextrin dimer facilitating cooperative inclusion of 2, 6-ANS, Beilstein Journal of Organic Chemistry 11 (2015) 514-523.
[62] V. Hildebrand, A. Laschewsky, M. Päch, P. Müller-Buschbaum, C.M. Papadakis, Effect of the zwitterion structure on the thermo-responsive behaviour of poly (sulfobetaine methacrylates), Polymer Chemistry 8(1) (2017) 310-322.
[63] H.S. Choi, T. Ooya, S. Sasaki, N. Yui, Control of rapid phase transition induced by supramolecular complexation of β-cyclodextrin-conjugated poly (ε-lysine) with a specific guest, Macromolecules 36(14) (2003) 5342-5347.
[64] N. Gonsior, H. Ritter, UCST Behavior of Cyclodextrin-Containing Poly (Pseudo-Betaines) Based on Supramolecular Structures, Macromolecular Chemistry and Physics 213(4) (2012) 382-388.

Highlights

- A β-cyclodextrin monomer is synthesized with excellent yield using "click" chemistry
- An ATRP protocol for the direct synthesis of sulfobetaine and β-cyclodextrin (co)polymers is presented
- Low size distributions ($Đ_M$) and high initiator efficiencies are obtained
- Excellent host-guest binding properties of the copolymers is revealed
- The copolymer shows salt-dependent UCST behavior

Graphical abstract